J Electroceram (2009) 23:209–213
DOI 10.1007/s10832-007-9395-9

Thermal and dielectric properties of glass-ceramics sintered based on diopside and anorthite composition

Jinho Kim · Seongjin Hwang · Wookyung Sung · Hyungsun Kim

Received: 31 May 2007 / Accepted: 11 December 2007 / Published online: 30 December 2007
© Springer Science + Business Media, LLC 2007

Abstract To develop a low dielectric constant of LTCC substrate, we studied the effect of the sintering and crystallization behavior on the dielectric properties of a sintered body by mixing a $CaO–Al_2O_3–SiO_2$ frit and a $CaO–MgO–SiO_2$ frit for a low dielectric constant of LTCC substrates. In this work, the two glass frits were mixed at different proportions and sintered at 860~920°C. After sintering at 900°C for 1h, the glass frits crystallized into diopside and anorthite. The sintered bodies exhibited dielectric properties, ε_r=6~8.6 at 1 GHz, which is an essential condition for a substrate in microwave devices. The results suggest that the glass-ceramic can be applied to low dielectric LTCC materials in the electronics packaging industry.

Keywords LTCC · Dielectric properties · Glass-ceramic · Crystallization

1 Introduction

Due to the increasing use of multimedia functions and the advances in the electronics industry, it is essential that electronic devices be miniaturized, lightweight, and highly efficient. Accordingly, the role of microwave equipment is becoming important for processing large-capacity information. There is a considerable amount of microwave equipment, such as cell-phones (0.9~1.8 GHz), GPS (global positioning system; 1.5 GHz), WLAN (wireless local area network), Bluetooth (2.4 GHz) and satellite communications (dozen of GHz) [1, 2]. These electronic devices have been developing using several packaging technologies including SoP (system-on-a-package), MCM (multi-chip module) and SMD (surface mounting device) [3–6].

Low temperature co-fired ceramic (LTCC) technology, which can be fired at low temperatures (<1000°C) using low melting temperature conductors, such as Cu (1083°C) and Ag (961°C), has received renewed attention [7–10]. Glass-ceramics can be used in multifunctional ceramic substrates with a low dielectric constant, high strength and low coefficient of thermal expansion. Glass-ceramics are expected to have the required properties because the dielectric properties can be easily controlled and the material has excellent mechanical strength. Generally, LTCC materials are divided into two classes: a substrate material with a low dielectric constant (below 10); and an embedded capacitor material that is suitable for multi-functions and has an intermediate or high dielectric constant [5, 6].

There have been many studies on low temperature fired substrate materials in the following systems: alumina–borosilicate glass [7], alumina–lead borosilicate glass [8], $MgO–Al_2O_3–SiO_2$ glass [9, 10] and $La_2O_3–B_2O_3–TiO_2$ [11]. A study on the $CaO–MgO–SiO_2$ glass system [12, 13] revealed high strength and low dielectric loss of the glass-ceramic substrate. The $CaO–Al_2O_3–SiO_2$ system [14] has been recently reported to have a low coefficient of thermal expansion, low dielectric constant and good chemical durability. However, the mechanical properties and dielectric properties are affected by the high porosity and low crystallinity of the glass-ceramic. The dielectric and mechanical characteristics of glass-ceramic, which has a complex microstructure, should be controlled by the porosity and degree of crystallization.

J. Kim · S. Hwang · W. Sung · H. Kim (✉)
School of Materials Engineering, Inha University,
253 Younghyun-dong, Nam-gu,
Incheon 402-751, Korea
e-mail: kimhs@inha.ac.kr

The aim of this study is to improve the dielectric properties of glass-ceramics by mixing two different frit compositions with a certain mixing proportion for applications to LTCC technology. This study examined the effect of the sintering and crystallization behavior on the dielectric properties of the sintered body by mixing a $CaO–Al_2O_3–SiO_2$ frit and a $CaO–MgO–SiO_2$ frit for a low dielectric constant of LTCC substrates.

2 Experimental procedures

The raw materials used for the glass frits were high purity $50SiO_2–15Al_2O_3–17CaO–11MgO–3Na_2O–4Fe_2O_3$ (AD1, in wt%) and $40SiO_2–30Al_2O_3–22CaO–8B_2O_3$ (AD2, in wt%; Aldrich, USA). The batches were melted in a platinum crucible at 1500°C for 3 h. The glass melts were poured quickly and quenched on a ribbon roller. The cullets were pulverized using a planetary mono mill (Pulverisette 5, Fritsch, Germany) for 7 h. The AD1 and AD2 frits (30:70 wt%, AD1: d_{50} −1.4 μm and AD2: d_{50} −1.7 μm) were mixed using a ball mill for 24 h and dried at 130°C for 24 h (AD3). Pellets (20 mm in diameter) were made by uniaxial pressing (62 MPa). The pellets were sintered at temperatures ranging from 860 to 920°C for 1 h at a heating rate of 10°C/min.

The particle size distribution of the powder was determined using a particle size analyzer (LS230 & N4PLUS, Coulter Corporation, USA). The glass transition temperature (T_g), the onset point of crystallization (T_c), and the crystallization peak (T_p) were determined using differential thermal analysis (DTA, TG 8120, Rigaku Co, Japan) at a heating rate of 10°C/min. Glass fibers, 0.5~0.75 cm in diameter and 23.5 cm in length, were made form the glass for the T_s test (Littleton softening point), which is the point at which the fiber elongates under its own weight at a rate of 1 mm/min. The shrinkage of samples was measured using a dilatometer (DIL402 PC, Netzsch Instruments, Selb, Germany).

The microstructures of the sintered sample were characterized by scanning electron microscopy (SEM, HITACHI, Japan). The porosity was measured by several SEM images with counting the pores. The crystal size and crystallinity of the sintered samples was determined from the SEM images of the etched samples. The phase constituents of the sintered body were examined by X-ray powder diffraction (XRD, Rigaku DMAX 2500, Japan). The dielectric constant and quality factor of the sintered sample were measured at room temperature using a RF impedance analyzer (E4991A, Agilent, USA) at a frequency of 1 GHz.

3 Results and discussion

Glass transition temperatures (T_g) of AD1, AD2 and AD3 are shown in Fig. 1. The T_g of AD1 is lower than that of AD2. In the case of AD3, which was prepared using a certain mixing proportion of AD1 and AD2, the T_g of AD3 has two glass transition temperatures, which are the same as the individual T_gs of AD1 and AD2. This suggests that the compositions of AD1 and AD2 should be unchanged in AD3.

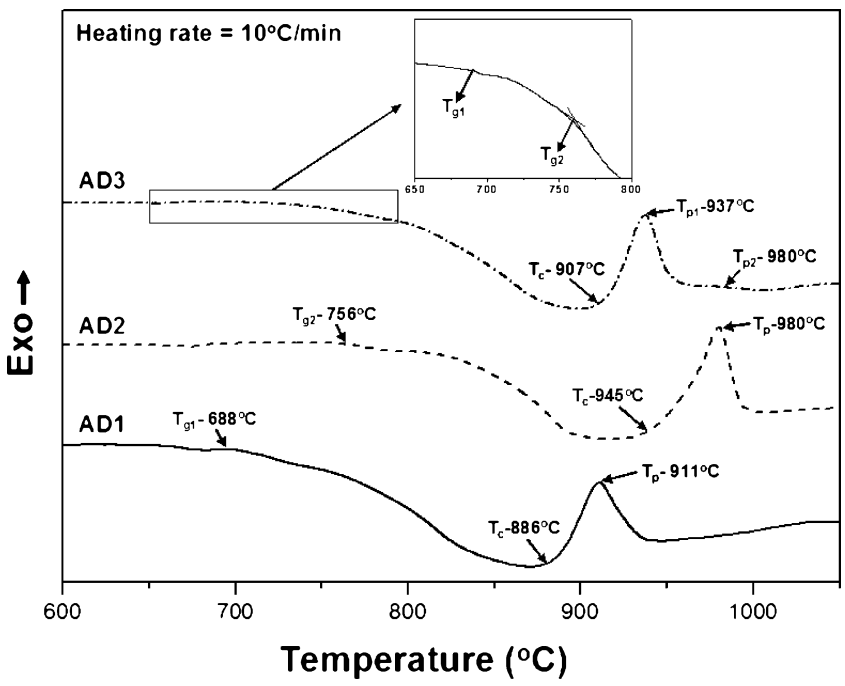

Fig. 1 DTA curves for frits and mixed frits heated at heating rate of 10°C/min

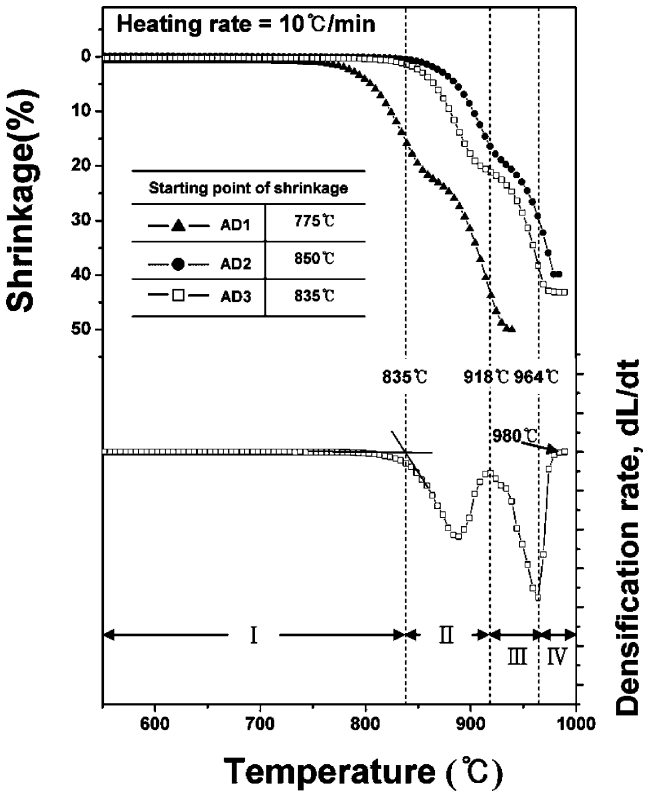

Fig. 2 Shrinkage of the frits (AD1, AD2 and AD3) and densification rate of the AD3 frit with increasing temperature

Furthermore, DTA curves for AD1, AD2 and AD3 show different exothermal peak temperatures, which mean the temperature of crystallization in glass (Fig. 1). The T_c of AD3 is in the middle range of the T_c of AD1 (T_c=886°C) and AD2 (T_c=945°C). After this temperature, two exothermic peaks (T_{p1} and T_{p2}) are observed in the AD3. Based on the DTA results, the two crystal phases can be generated by AD1 and AD2 in the AD3. Considering that the two frits were mixed physically, it is believed that AD1 acts as a sintering agent in the matrix and controls the temperature of crystallization.

From the result of shrinkage, the possibility of sintering at 900°C is considered due to the low T_s ($\eta=10^{7.6}$ dPa), which is at 818°C (AD1) and 868°C (AD2). The starting point of shrinkage (T_{ss}) for the glass frits occurs at a temperature considerably lower than 900°C, as shown in Fig. 2. Shrinkage of the AD1, AD2 and AD3 samples begin at 775, 850 and 835°C, respectively. The shrinkage of the glass frits is approximately 40~50%, which is attributed to the low viscosity of the glass. The difference in shrinkage can be due to the difference thermal properties (T_g, T_s and

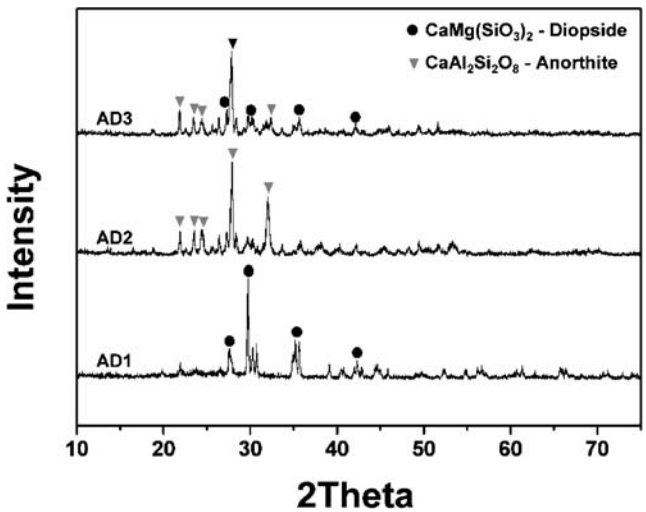

Fig. 3 XRD patterns of the glass frits (AD1, AD2) and mixed glass frits (AD3) fired at 900°C for 1 h

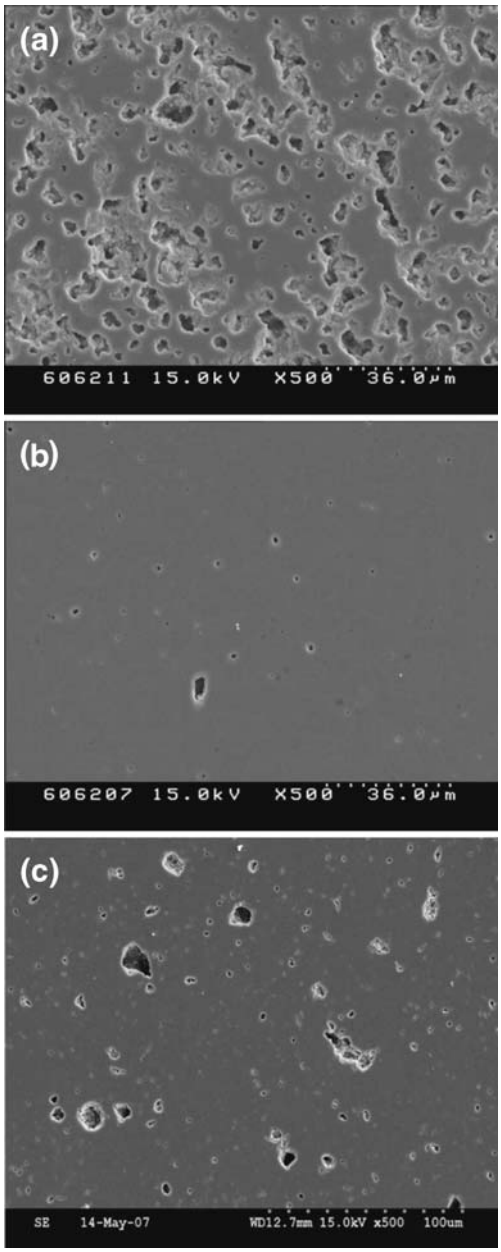

Fig. 4 SEM images of the glass frits and mixed glass frit sintered at 900°C for 1 h (**a**) AD1, (**b**) AD2 and (**c**) AD3

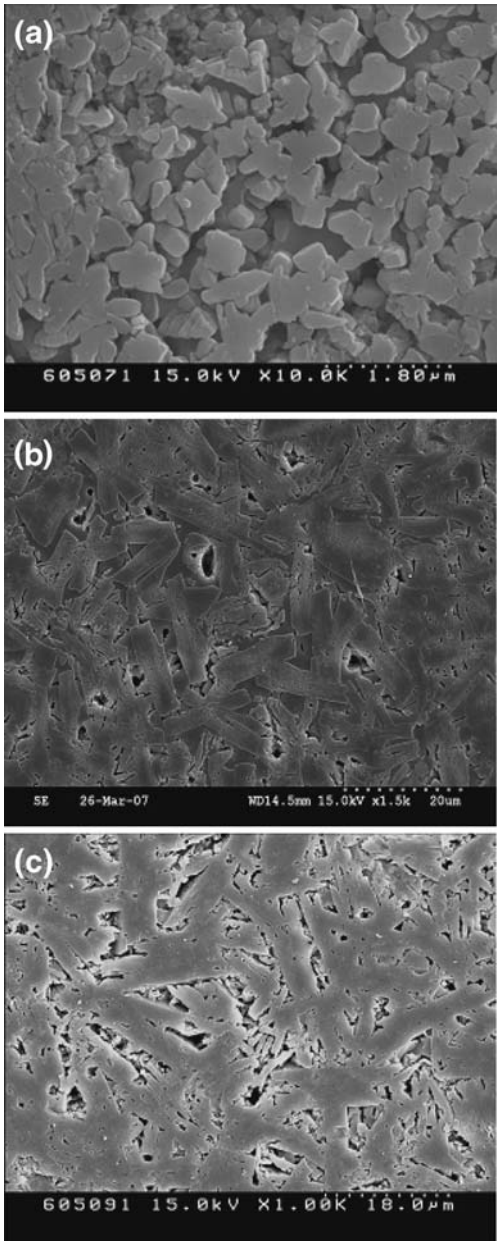

Fig. 5 Typical etched microstructures of the glass-ceramics sintered with the glass frits and the mixed glass frit at 900°C for 1 h (**a**) AD1, (**b**) AD2 and (**c**) AD3. [Etching condition: (**a**) 5% HF for 30 sec, (**b**) and (**c**) 5% HNO_3 for 15 min]

T_c). However, the T_{ss} of AD3 is somewhere between T_{ss} of AD1 and AD2 frits. Based on the thermal properties (Figs. 1 and 2), AD1 may have acted as a sintering agent in AD3 during crystallization.

For the shrinkage and the densification rate of AD3, 4 sections could be identified in terms of the densification rate (Fig. 2). In the first and fourth (I, IV) section in Fig. 2, the AD3 shows no change in the shrinkage. However, the AD3 shrinks with a different densification rate in sections second (II) and third (III), as shown in Fig. 2. This is attributed to the content of AD1 and AD2 in AD3.

Table 1 Porosity, pore size, crystallinity and crystal size of the sintered bodies (AD1, AD2, and AD3) at 900°C for 1 h.

Sample	Porosity (%)	Pore size (μm)	Crystallinity (%)	Crystal size (μm)	
				Diopside	Anorthite
AD1	16±2.5	<13	105±9.3	0.6±0.1	–
AD2	5.8±1.2	<4	87.6±2.3	–	15.4±3.0
AD3	7.9±2.4	<10	87.7±7.7	0.5±0.2	14.2±2.5

Furthermore, if AD3 crystallizes in two crystalline phases at different temperatures, the densification rate is related to the temperature of crystallization as well as to the grain growth of the crystalline phases [14]. Therefore, the different densification rate between the second and third section with AD3 need to be considered with the contents of AD1 and AD2 as well as the T_c and T_p of the frits.

From the XRD patterns, the AD3 sintered at 900°C for 1 h contains two crystalline phases, $CaMg(SiO_3)_2$ (diopside, JCPDS No. 11-0654) and $CaAl_2Si_2O_8$ (anorthite, JCPDS No. 03-0505) (Fig. 3). Furthermore, the AD1 and AD2 samples sintered at 900°C for 1 h contains diopside and anorthite, respectively. A comparison with the DTA results (Fig. 1) shows that the two exothermic peaks of AD3 corresponded to the formation of the diopside and the anorthite, respectively. As mentioned previously, the formation of these crystalline phases (diopside and anorthite) can interrupt shrinkage and the densification.

Pores were formed in the sintered bodies during the formation of diopside or anorthite (Fig. 4). The shape of the pores in the sintered body of AD1 is irregular and large (<13 μm). This suggests that the diopside in AD1 has high crystallinity after sintering at 900°C for 1 h. In the sintered body of AD1 there is low amount of residual glass, which can occupy the pores. At temperatures higher than the fusion temperature, the source of the pores is the formation

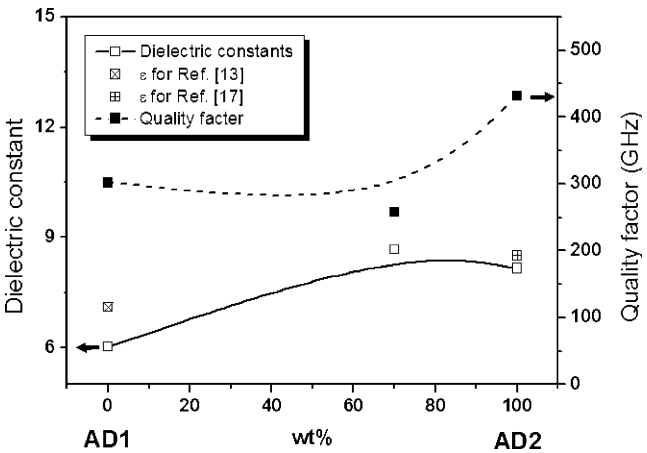

Fig. 6 Dielectric constant and quality factor of the sintered frits with different compositions. (Sintering condition: 900°C for 1 h at1 GHz)

of crystallization [15]. In contrast to AD1, the sintered body of AD2 at 900°C for 1 h has low porosity (~5%). The difference in porosity in the sintered bodies between AD1 and AD2 is affected by the degree of crystallization. In the case of AD3, small and spherical pores are formed as a result of the formation of an anorthite phase after the irregular pores was formed by the diopside phase. This change in the pore size of AD3 is attributed to a difference in the starting temperature for densification and crystallization, which contributed to the difference in crystallinity.

Figure 5 shows SEM images of the sintered and etched AD1, AD2 and AD3 samples. The shape of diopside and anorthite is round and rectangular, respectively, which might affect the dielectric properties of AD1, AD2 and AD3. Based on the SEM images, the crystallinity of the sintered bodies (AD1, AD2 and AD3) is 105±9.3, 87.6± 2.3 and 87.7±7.7%, respectively. However, the crystallinity of sintered AD1 has a large error due to the size of the crystalline phase and large pores (Table 1).

The dielectric constant and quality factor of the samples increase slightly with increasing AD2 content (Fig. 6). The dielectric constant of the material is dependent on the porosity, crystalline phase size, direction and distribution of grains and density [16]. The dielectric constant of AD3 sintered at 900°C for 1 h increases as a result of the lower porosity and dielectric constants of the residual glass. The dielectric constant for pure anorthite with a relative density of approximately 95% is 8.5 at 1 MHz [17]. Therefore, the dielectric constant of the residual glass is believed be higher than that of anorthite.

However, the dielectric constant of sintered AD1 is lower than reported elsewhere [13]. The reason might be the porosity and pore size of AD1 sintered at 900°C for 1 h. The dielectric constant decreases with increasing porosity in the materials because the dielectric constant of a pore is 1 [18]. A comparison of the dielectric constant of AD2 sintered with previous research [17] (k≈8.5 at 1 MHz) suggests that the low value is associated with the porosity and the dielectric constant of the residual glass. The theoretical dielectric constant of AD1 and AD2 is 7.4 and 8.8, respectively according to the Rayleigh model [19].

In general, the quality factor is affected mainly by the pore size, the crystal phase, the mean crystal size and the crystallinity [16, 18]. The quality factor of AD1 is lower than AD2 (Fig. 6). This results from the small size of the crystal phase (0.5 μm) and large pore size (13 μm). However, the quality factor of AD3 is lowest in the three samples after sintering at 900°C for 1 h. This suggests that the quality factor of AD3 is influenced by an interaction between the residual glass, diopside and anorthite.

4 Conclusion

This study examined the thermal and dielectric properties of a glass-ceramic with a complex microstructure with two types of glass frit ($CaO–Al_2O_3–SiO_2$ and $CaO–MgO–SiO_2$ system). There is a correlation between the porosity of the mixed crystal phases and the dielectric properties in the glass-ceramic. A mixture of different frits contributed to the high densification and low dielectric constants. Therefore, we suggest that the dielectric constants and microstructure of a glass-ceramic can be controlled by the ratio of the two glasses in the mixture, $CaO–Al_2O_3–SiO_2$ and $CaO–MgO–SiO_2$ systems. Furthermore, this material is a candidate for optimal LTCC substrate materials.

Acknowledgement This work was supported by the IT R&D program of MIC/IITA (2006-s055-02, Ceramic Material and Process for High Integrated Module).

References

1. J.Y. Ha, J.W. Choi, C.Y. Kang, S.J. Yoon, D.J. Choi, H.J. Kim, J. Electrocerams. **17**, 399–403 (2006)
2. C.L. Huang, Y.C. Chen, J. Euro. Ceram. Soc. **23**, 167–173 (2003)
3. J.L. Sprague, IEEE Trans. Comp. Hyb. Manuf. Tech. **13**, 390–396 (1990)
4. R.R. Tummala, J. Am. Ceram. Soc. **74**, 895–908 (1991)
5. R. Umemura, H. Ogawa, A. Yokoi, H. Ohsato, A. Kan, J. Alloys. Compd. **424**, 388–393 (2006)
6. Q. Zeng, W. Li, J.L. Shi, J.K. Guo, M.W. Zuo, W.J. Wu, J. Am. Ceram. Soc. **89**, 1733–1735 (2006)
7. R.C.C.C. Monteiro, M.M.R.A. Lima, J. Euro. Ceram. Soc. **23**, 1813–1818 (2003)
8. K.P. Kumar, V.C.S. Prasad, P.S. Mukherjee, P.G. Mukunda, Mater. Sci. Eng. **B5**, 1–4 (1989)
9. G. Chen, X. Liu, Mater. Sci. **15**, 595–600 (2004)
10. L. Luo, H. Zhou, C. Xu, Mater. Sci. **13**, 381–386 (2002)
11. S.J. Hwang, Y.J. Kim, H.S. Kim, J. Electrocerams. **18**, 121–128 (2007)
12. A. Karamanov, L. Arrizza, I. Matekovits, M. Pelino, Ceram. Inter. **30**, 2129–2135 (2004)
13. K. Hayashi, Y. Nishioka, Y. Okamoto, J. Ceram. Soc. Jap. **98**, 801–805 (1990)
14. C.L. Lo, J.G. Duh, B.S. Chiou, J. Mater. Sci. **38**, 693–693 (2003)
15. S. Hwang, H. Kim, Thermochimica Acta **455**, 119–122 (2007)
16. M. Valant, D. Suvorov, Mat. Chemistry and Physics **79**, 104–110 (2003)
17. M.G.M.U. Ismail, H. Arai, J. Ceram. Soc. Jap. **100**, 1385–1389 (1992)
18. S.J. Penn, N.M. Alford, A. Templeton, X. Wang, M. Xu, M. Reece, K. Schrapel, J. Am. Ceram. Soc. **80**, 1885–1888 (1997)
19. R.W. Rice, Porosity of Ceramics (Marcel Dekker Inc., Virginia, 1998), p. 328